Available online at www.sciencedirect.com
SCIENCE DIRECT
ELSEVIER
Polymer 46 (2005) 5140–5148
polymer
www.elsevier.com/locate/polymer

Langmuir and Langmuir-Blodgett (LB) films of poly[(2-methoxy,5-*n*-octadecyl)-*p*-phenylenevinylene] (OC_1OC_{18}-PPV)

Marystela Ferreira[a,*], Carlos J.L. Constantino[a], Clarissa A. Olivati[a], Débora T. Balogh[b], Ricardo F. Aroca[c], Roberto M. Faria[b], Osvaldo N. Oliveira Jr[b]

[a]*Depto de Física, Química e Biologia, Faculdade de Ciências e Tecnologia, Universidade Estadual Paulista, CP 467, 19060-900 Presidente Prudente, SP, Brazil*
[b]*Instituto de Física de São Carlos, Universidade de São Paulo, CP 369, 13560-970 São Carlos, SP, Brazil*
[c]*Materials and Surface Science Group, School of Physical Sciences, University of Windsor, Windsor, ON, Canada N9B 3P4*

Received 16 December 2004; received in revised form 18 April 2005; accepted 20 April 2005
Available online 10 May 2005

Abstract

A PPV derivative, poly(2-methoxy,5-(*n*-octadecyl)-*p*-phenylenevinylene) (OC_1OC_{18}-PPV), has been synthesized via the Gilch route and used to fabricate Langmuir and Langmuir-Blodgett (LB) films. True monomolecular films were formed at the air/water interface, which were successfully transferred onto different types of substrate. Using UV–visible absorption, FTIR, fluorescence and Raman scattering spectroscopies we observed that the polymer molecules were randomly distributed in the LB film, with no detectable anisotropy. This is in contrast to the anisotropic LB films of a previously reported PPV derivative, poly(2-methoxy-5-*n*-hexyloxy)-*p*-phenylenevinylene (OC_1OC_6-PPV), which is surprising because the longer chain of OC_1OC_{18}-PPV investigated here was expected to lead to more ordered films. As a consequence of the lack of order, LB films of OC_1OC_{18}-PPV exhibit lower photoconductivity and require higher operating voltage in a polymer light-emitting diode (PLED) in comparison with LB films of OC_1OC_6-PPV. This result confirms the importance of molecular organization in the LB film to obtain efficient PLEDs.

Keywords: Langmuir-Blodgett films; Light-emitting diode; PPV

1. Introduction

Molecular engineering strategies have been developed over the years to obtain luminescent devices with the required emission properties [1,2], including color [1,2] and polarization [1,2]. For luminescent polymers, in particular, the first step in such strategies is the chemical synthesis of innovative polymers, which may be display enhanced emission. In the poly(*p*-phenylene vinylene) (PPV) family, derivatives have been synthesized containing alkyl chains, making them soluble in organic solvents [3]. Another degree of molecular control can be achieved by employing film fabrication techniques where the polymer chains may be deposited in a layer-by-layer fashion, as in the case of Langmuir-Blodgett (LB) [4] and electrostatically assembled layer-by-layer (LbL) films [4]. The main feature of these films is polarized emission owing to film anisotropy. A few reports have been made of LB films from PPV derivatives [5–9]. Sluch et al. [5] studied the photo and electroluminescence properties of LB films from poly(2-methoxy-5-(2′-ethylhexyloxy)-*p*-phenylenevinylene), MEH-PPV. Jung et al. [8,9] used MEH-PPV LB films as the emitting layer to improve the quantum efficiency of light-emitting diodes (LEDs). Wu et al. [7] investigated the LB film characteristics of poly[2-methoxy-5-(2′-*n*-hexadecyloxy)-*p*-phenylenevinylene] using UV–visible polarized spectroscopy and linear dichroism infrared analysis and showed that the polymer chains exhibited some degree of orientation. For Langmuir and LB films from poly(2-methoxy-5-(2′-*n*-hexadecyloxy)-*p*-phenylenevinylene), Wu et al. [6] suggested on the basis of atomic force microscopy (AFM) images and UV polarized spectra that the film exhibits the main chains aligned in the LB dipping direction. Molecular organization has been shown to improve the optical

* Corresponding author. Tel.: +55 182 295 355; fax +55 182 215 682.
E-mail address: mstela@prudente.unesp.br (M. Ferreira).

0032-3861/$ - see front matter © 2005 Elsevier Ltd. All rights reserved.
doi:10.1016/j.polymer.2005.04.037

properties of thin films from PPV derivatives [10,11], which also occurs for LB films from thermally converted PPV [12].

In a previous paper we studied Langmuir and LB films of the PPV derivative poly(2-methoxy-5-*n*-hexyloxy)-*p*-phenylenevinylene (OC_1OC_6-PPV) [13]. The FTIR spectra for the LB films showed that the OC_1OC_6-PPV molecules are attached to the substrate surface by the lateral groups ($R_1 = OC_1$ or $R_2 = OC_6$). Combining FTIR and Raman scattering data, we inferred that the vinylic C–H group was almost parallel to the substrate surface. The LB films displayed spectroscopic, fluorescence and electrochemical properties that were remarkably different from those of cast films of OC_1OC_6-PPV, probably due to the molecular organization in the LB films. Anisotropy was confirmed with polarized photoluminescence [14]. The organized LB films were then exploited in the fabrication of polymer LEDs (PLEDs), which exhibited a relatively low operating voltage (ca. 5 V) [15].

The remarkable properties of LB films from OC_1OC_6-PPV pointed to the possible importance of molecular ordering in the LB films. In order to probe this hypothesis, one possibility is to employ similar PPV derivatives with different chain lengths. In particular, a PPV derivative with a longer hydrophobic side chain would be expected to facilitate LB film formation, in analogy with that observed in carboxylic acids [16]. For this work, we have synthesized poly(2-methoxy,5-(*n*-octadecyl)-*p*-phenylenevinylene) (OC_1OC_{18}-PPV), whose structure is shown in the inset of Fig. 1. OC_1OC_{18}-PPV is used to produce Langmuir and LB films, in addition to cast films. LB and cast films are characterized with UV–visible absorption, FTIR in transmission and reflection-absorption (RAIRS = reflection absorption infrared spectroscopy) modes, Raman scattering, fluorescence and conductivity measurements. In contrast to our expectation, the longer side chain leads to isotropic films in terms of molecular structure. As will be shown, this affects the performance of PLED devices obtained with LB films.

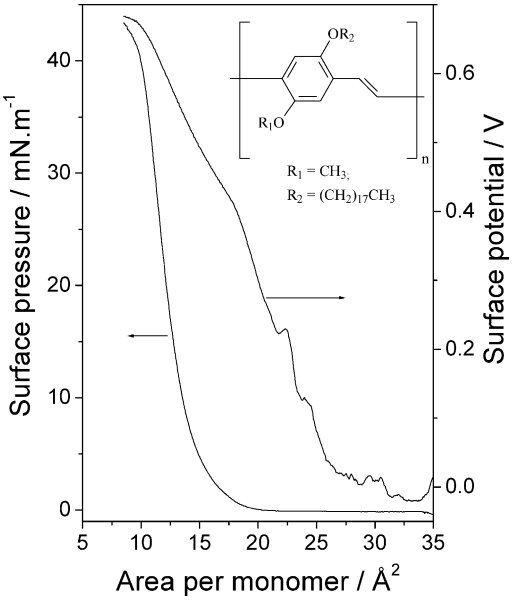

Fig. 1. Surface pressure-area and surface potential-area isotherms for pure OC_1OC_{18}-PPV on a pure water subphase. $T = 22$ °C.

2. Experimental details

The polymer OC_1OC_{18}-PPV was synthesized using a procedure similar to that described in Ref. [3]. The molecular weight (M_w) of this polymer is ca. 8×10^5 g/mol, with a degree of polymerization of approximately 2000 as determined by HPSEC in an Agilent 1100 chromatographic system, with 1 ml/min of tetrahydrofuran as eluent and polystyrene standards. The temperature of initial (T_{id}) of the thermal degradation was determined by thermogravimetric analysis in a NETSCH TG 290, using ca. 3.8 mg of the sample at heating rate of 10 °C /min from ambient to 1000 °C, under nitrogen atmosphere. For the Langmuir and LB experiments, OC_1OC_{18}-PPV was dissolved in chloroform (0.2 mg ml^{-1}) and the films were produced with a KSV 5000 Langmuir trough housed in a class 10,000 clean room. Langmuir films were spread onto ultra pure water obtained from a Millipore Milli-Q system (resistivity 18.2 MΩ cm), with compression carried out at a barrier speed of 10 mm min^{-1}. All experiments were conducted at room temperature (22 °C). π–A and ΔV–A isotherms were performed with a Wilhelmy plate and a Kelvin probe, respectively, both provided by KSV. Stability measurements of the Langmuir films were obtained by keeping the surface pressure at 30 mN m^{-1} while the time evolution of the area per monomer was recorded, and by performing successive cycles of compression–decompression of the films. The molecular weight of the polymer-repeating unit (400 g mol^{-1}) was adopted for all area calculations.

LB films were produced by transferring pure OC_1OC_{18}-PPV Langmuir films onto one of the following substrates: glass or glass coated with ITO (Asahi Glass Co., Japan), interdigitated electrodes of chromium–gold array, and silicon wafers (Aldrich). Y-type LB films either with 25 or 51 layers were transferred at a surface pressure of 30 mN m^{-1} with a typical dipping speed of 3 mm min^{-1} for the upstroke and downstroke. The transfer ratio (TR) for the LB films was ca. 0.9 in the upstrokes and 0.7 in the downstroke. A 25-layer LB film was characterized by FTIR spectroscopy either in the transmission mode on silicon wafers using a ThermoNicolet Nexus 470, 4 cm^{-1} spectral resolution and 64 scans, or in RAIRS mode on Ag mirrors using a BOMEM DA3, MCT detector, 4 cm^{-1} spectral resolution, 1032 scans, 80° incident angle, and evacuating the sample chamber to 0.5 Torr. The Raman scattering and emission spectra were recorded with the laser lines at 633 and 514.5 nm using a Renishaw Research Raman Microscope System RM2000 equipped with a Leica microscope (DMLM series), 1800 grooves/mm grating, spectral

resolution of ca. 3 cm^{-1} and a Peltier cooled (−70 °C) CCD array detector. The spectra were also collected at different temperatures from −100 to +200 °C using a Linkan 600 temperature stage. The Raman spectra at room temperature (ca. 22 °C) were collected using the 50× objective, 3 accumulations and 1 s collecting time while the emission spectra at room temperature were collected using a 5×objective lens (100% defocused), 1 accumulation and 1 s collecting time. Both Raman and emission spectra as a function of the temperature were recorded using the 50×-long objective, 3 accumulations for Raman and 1 accumulation for emission and 1 s collecting time. In all cases the laser power at the sample was in the μW level. Data acquisition and analysis were carried out using the WIRE software for Windows and Galactic Industries GRAMS/32™. UV–visible absorption measurements were carried out in a HITACHI U-2001 spectrophotometer in the range between 350 and 800 nm. All the film formation studies and characterizations were carried out in the dark to prevent photo-oxidation.

For the electrical measurements a 81-layer LB film of OC_1OC_{18}-PPV was deposited on a glass substrate coated with an interdigitated chromium–gold array, whose fabrication is described in detail elsewhere [13,17]. The electrical characterization was carried out using a Keithley 238 (High Source Voltage Unit) in the dark and under illumination at room temperature.

The device made with a LB film of OC_1OC_{18}-PPV was fabricated as follows. A 51-layer LB film was deposited onto ITO that had been previously cleaned according to the procedures of Ref. [18]. A 90 nm thick Al cathode was vacuum evaporated (10^{-6} Torr) on top of the LB film, leading to a final structure ITO/OC_1OC_{18}-PPV/Al, and with an active area for the devices of 0.12 cm^2.

3. Results and discussion

3.1. Langmuir films of OC_1OC_{18}-PPV

Fig. 1 shows the π–A and ΔV–A isotherms of pure OC_1OC_{18}-PPV film, featuring a collapse pressure of ca. 40 mN m^{-1} and an extrapolated area of approximately 18 $Å^2$ per monomer for the condensed phase in the π–A isotherm, calculated using the molecular weight of the polymer-repeating unit. This value is close to that obtained for OC_1OC_{18}-PPV in the CPK model using Hyperchem program (~23 $Å^2$), indicating the formation of monomolecular structures. Aggregation, if present, occurs at a very limited extent. The area of 18 $Å^2$ is similar to the one obtained by Ferreira et al. for OC_1OC_6-PPV [13], i.e. approximately 22–25 $Å^2$, which means that the aromatic and vinyl groups are oriented perpendicularly to the water surface. The formation of true monolayer was also observed for poly[(2-methoxy-5-*n*-hexaloxy)-*p*-phenylenevinylene] with 16 carbons (MH-PPV) [7]. Only MEH-PPV (poly[2-methoxy,5-(2′-ethylhexyloxy)-*p*-phenylenevinylene]) (MEH-PPV) did not form monolayers (extrapolated area of only ca. 2.7 $Å^2$) [5]. It seems that the linearity of the side-chain must play an important role since the linear side chain polymers (OC_1OC_6-PPV and MH-PPV) formed true monolayers, but the branched one (MEH-PPV) did not. Stability for the Langmuir films from OC_1OC_{18}-PPV was attained in hysteresis measurements after 2 compression-decompression cycles, with the π–A isotherms being the same in subsequent runs. The stability was confirmed in experiments where the surface pressure was kept at 30 mN m^{-1}, with small decreases in area per monomer of 3 and 10% after 1 h and 3 h, respectively. The large surface potential, i.e. approximately 700 mV, for the condensed phase indicates the contribution of large dipole moments in the OC_1OC_{18}-PPV as expected in the case of the molecule placed perpendicularly to the water surface.

3.2. Characterization of OC_1OC_{18}-PPV LB films

The polarized absorption spectra of a 25-layer LB film from OC_1OC_{18}-PPV deposited onto glass are displayed in Fig. 2 for two polarizations of the incident light, viz. parallel ($A_{\parallel}$) and perpendicular ($A_{\perp}$) to the dipping direction. The absorption band with maximum at ca. λ_{max} 495 nm is related to transitions between delocalized π–π* states. UV–visible absorption due to conjugated segments is very sensitive to the direction of polarization of an incident light, which enables the use of polarized light to probe structural film anisotropy [19]. For LB films of this compound, the absorption was similar for the two directions, indicating a random molecular organization in the LB films. For the PPV derivative with 6 carbons, OC_1OC_6-PPV, the anisotropy was observed with polarized UV, FTIR and

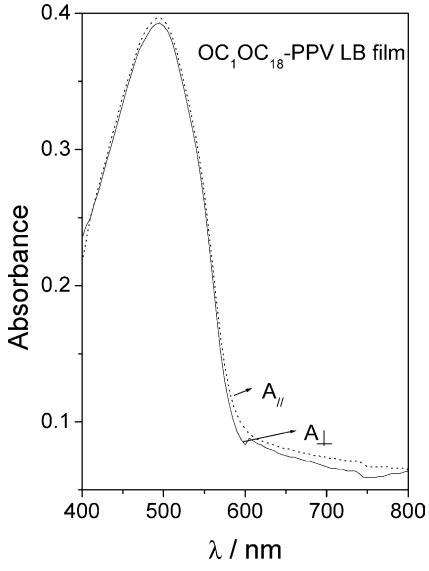

Fig. 2. Polarized absorption spectra at 25 °C for a 25-layer LB film for two polarizations of the incident light: parallel ($A_{\parallel}$) and perpendicular ($A_{\perp}$) to the dipping direction.

photoluminescence [13,14]. The dichroic ratio ($A_{\parallel}/A_{\perp}$) taken at the maximum of the π–π^* band was ca. 1.56 for a 41-layer OC_1OC_6-PPV LB film. Wu et al. [7] observed some anisotropy in LB films of MH-PPV (16 carbons in the lateral chain) with a dichroic ratio of ca. 1.10. Thus, these results indicate that the length of the lateral chain is an important parameter in the organization of the LB films.

Fig. 3 presents an optical image collected using the 5× objective for a 25-layer LB film of OC_1OC_{18}-PPV on glass, where the presence of aggregates in the micrometer scale is evident. The emission spectra from different spots (darker and lighter) of this film using the 514.5 nm as the excitation light were recorded. The emission is assigned to π–π^* transitions in the orbitals of the main chain with the vibronic structure of the emission spectra suggesting an intrachain transition [13]. It seems that the darker area in the optical image contains less material than the lighter one since the emission from the lighter area is consistently weaker (though not significantly). The emission spectra for the 514.5 nm excitation laser line for 1-layer OC_1OC_{18}-PPV LB film deposited onto Ag nanoparticle film (6 nm mass thickness) and the emission spectra for 1-layer OC_1OC_{18}-PPV LB film on glass were collected to check a possible surface enhanced fluorescence (SEF) [20] for this PPV derivative (figure not shown). However, no enhancement was observed, which suggests that either the molecules are placed face-down on to the surface with the main chain touching the Ag islands or they are randomly organized. Since there are two mechanisms competing here, enhancement and quenching of the fluorescence, the contact between the emitter group and the metal surface would produce fluorescence quenching rather than enhancement [21].

Fig. 4 presents the Raman spectra recorded with the 633 nm laser line for the 25-layer OC_1OC_{18}-PPV LB film from different areas of the surface as shown in the optical image using a 50×objective. The spectra are similar, indicating that there are no significant differences in the chemical composition from area to area. The differences in color presented in the optical image should be attributed to different amounts of material, which induce changes in the background spectra. This effect can be seen in Fig. 5, which shows a Raman mapping with the spectra being collected along a line of 70 μm (step of 2 μm). The line mapping is shown with and without baseline to highlight the background effect. In addition, a very weak band is seen at 970 cm^{-1} (Fig. 4), which demonstrates that the phenylene and the vinylene groups are practically in the same plane [22]. FTIR spectra collected in both transmission and reflection (RAIRS) [23] are shown in Fig. 6. Using the concept of local symmetry, the latter spectra can be used to determine the molecular organization of OC_1OC_{18}-PPV in LB films. The transmission spectrum of the bulk is taken as reference when extracting information about molecular organization since it represents a random distribution of molecular units in the bulk. The similarity between the spectra shows qualitatively that the molecules are also randomly distributed in the LB film. Specifically, the key normal modes at 850 and 970 cm^{-1} assigned to aromatic and vinyl C–H wagging [24], respectively, both perpendicular to the plane containing the phenylene and vinylene groups, have the same trend in terms of relative intensity for all cases.

Because the temperature may play an important role in molecular degradation and arrangement assumed for the molecules in the films, which are important parameters for

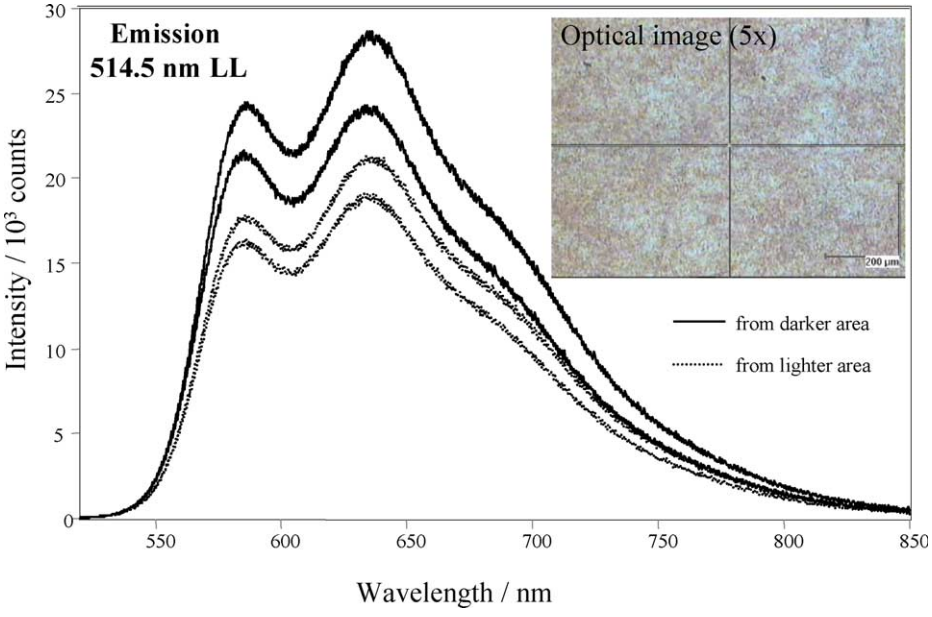

Fig. 3. Fluorescence spectra for a 25-layer LB film of OC_1OC_{18}-PPV. The inset shows the optical image (5×) of an area of the film; all other areas presented similar images.

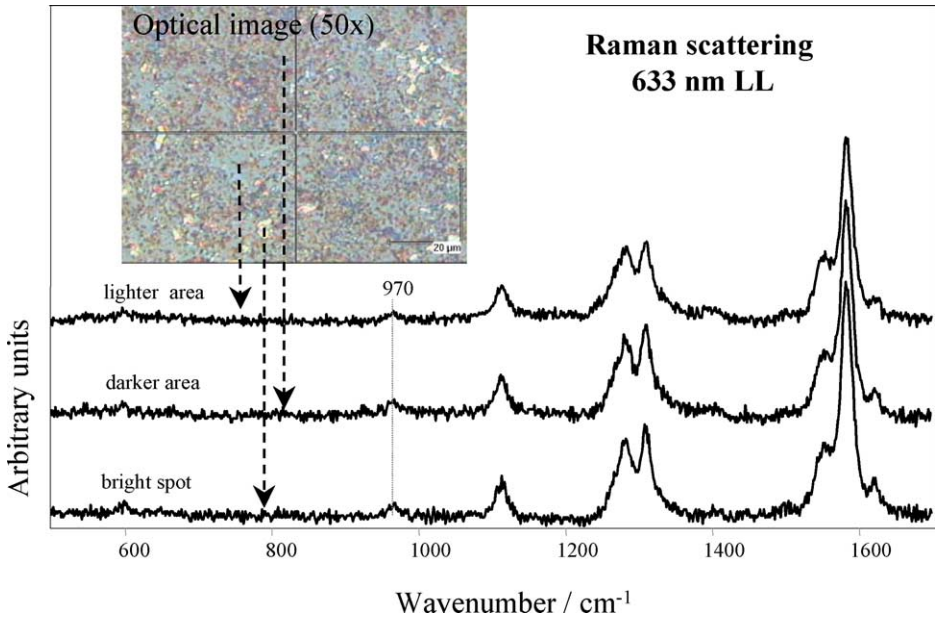

Fig. 4. Raman spectra for the 25-layer LB film of OC_1OC_{18}-PPV collected from different areas of the film, as indicated in the optical image in the inset.

luminescent devices, we measured emission and Raman scattering with LB films at various temperatures. Fig. 7 shows emission spectra using the 514.5 nm excitation laser line for the 25-layer LB film submitted to the following cyclic temperature program: $T_1 = +20\,^{\circ}C \rightarrow T_2 = -50\,^{\circ}C \rightarrow T_3 = -100\,^{\circ}C \rightarrow T_4 = -50\,^{\circ}C \rightarrow T_5 = +20\,^{\circ}C \rightarrow T_6 = +100\,^{\circ}C \rightarrow T_7 = +200\,^{\circ}C \rightarrow T_8 = +20\,^{\circ}C$. A blow up of the figure in the range between T_3 and T_8 is shown in the inset. The Raman spectra obtained with the 633 nm laser line for the 25-layer LB film, with the same temperature program, are shown in Fig. 8. Not all data are shown to avoid overcrowding the figure; for example, the spectra for $T_1 = +20\,^{\circ}C$ and $T_2 = -50\,^{\circ}C$ are not presented since they are very similar to T_5 and T_4, respectively. The inset in Fig. 8 shows the same Raman spectra from T_3 to T_8, but deliberately shifted to highlight the main features.

In the range between -100 and $+100\,^{\circ}C$ the emission spectra are reversible and maintain their vibronic structure, with the same overall profile. Therefore, neither the film structure nor the molecules are significantly affected by the increase and decrease in temperature in that range. The increase in intensity at lower temperatures for emission and Raman scattering are associated with the freezing of the molecular system. This allows a more intense emission

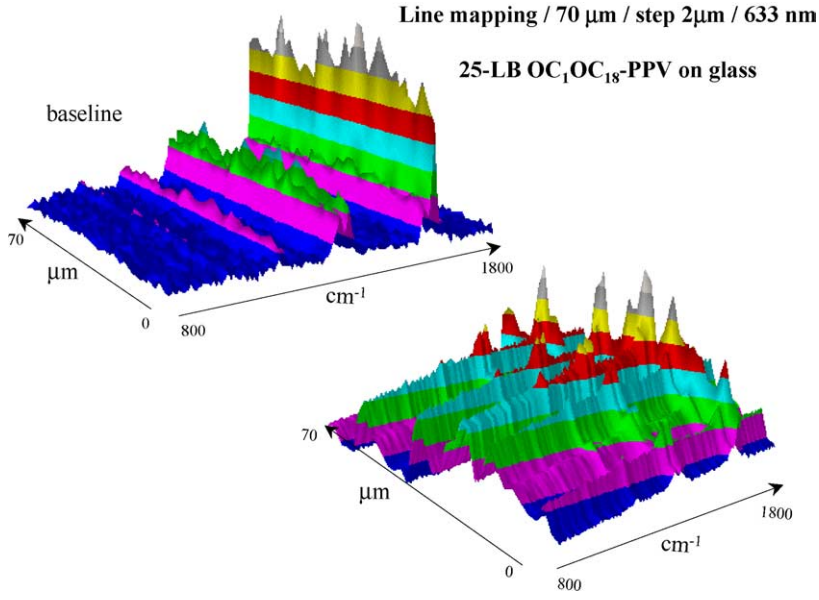

Fig. 5. Raman mapping without baseline correction with the spectra being collected along a line of 70 µm (step of 2 µm) for a 25-layer LB film of OC_1OC_{18}-PPV.

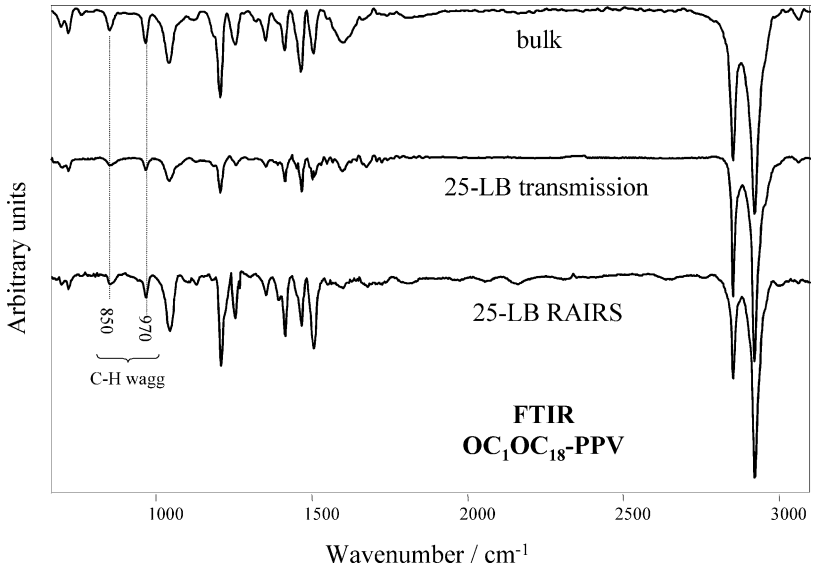

Fig. 6. FTIR transmission spectra for OC_1OC_{18}-PPV, as a bulk sample and 25-layer LB film, and RAIRS spectrum for the 25-layer LB film.

because the molecular relaxation to the electronic ground state through molecular motion is minimized, and a larger Raman scattering due to the reduction of the phonon background. At $T_7 = +200\,^{\circ}C$ the emission spectrum in Fig. 7 loses its vibronic structure, which may indicate some molecular degradation, although the thermogravimetric curve shown in Fig. 9 was almost flat up to the temperature where decomposition starts, at 280 °C. On the other hand, the Raman spectrum recorded at $T_8 = +20\,^{\circ}C$ after the film had reached $T_7 = +200\,^{\circ}C$ has the shape observed for temperatures lower than $T_7 = +200\,^{\circ}C$ (Fig. 8), which suggest that the film structure may be more affected by temperature in the range investigated than the molecular structure itself. This is supported by the partial recovery of the emission spectrum shape at $T_8 = +20\,^{\circ}C$. Nevertheless, the lowering in emission intensity means that heating up to 200 °C is sufficient to damage the film as far as applications in luminescent devices are concerned. In subsidiary experiments, the X-ray diffractogram for a 51-layer LB film deposited onto glass was obtained and no peaks were observed, which indicates the absence of crystallinity in the film.

3.3. PLEDs with the OC_1OC_{18}-PPV LB films

Polymer light emitting diodes were fabricated with LB films of OC_1OC_{18}-PPV sandwiched between ITO and aluminum electrodes and the conductivity measurements

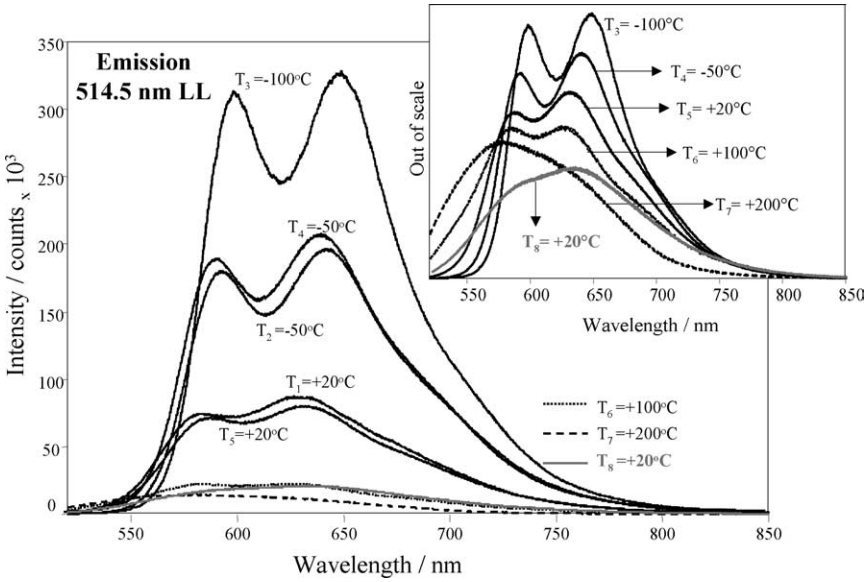

Fig. 7. Emission spectra for the 25-layer LB film submitted to the following cyclic temperature program: $T_1 = +20\,^{\circ}C \rightarrow T_2 = -50\,^{\circ}C \rightarrow T_3 = -100\,^{\circ}C \rightarrow T_4 = -50\,^{\circ}C \rightarrow T_5 = +20\,^{\circ}C \rightarrow T_6 = +100\,^{\circ}C \rightarrow T_7 = +200\,^{\circ}C \rightarrow T_8 = +20\,^{\circ}C$. The inset blows up the spectra from T_3 to T_8. Excitation laser line is 514.5 nm.

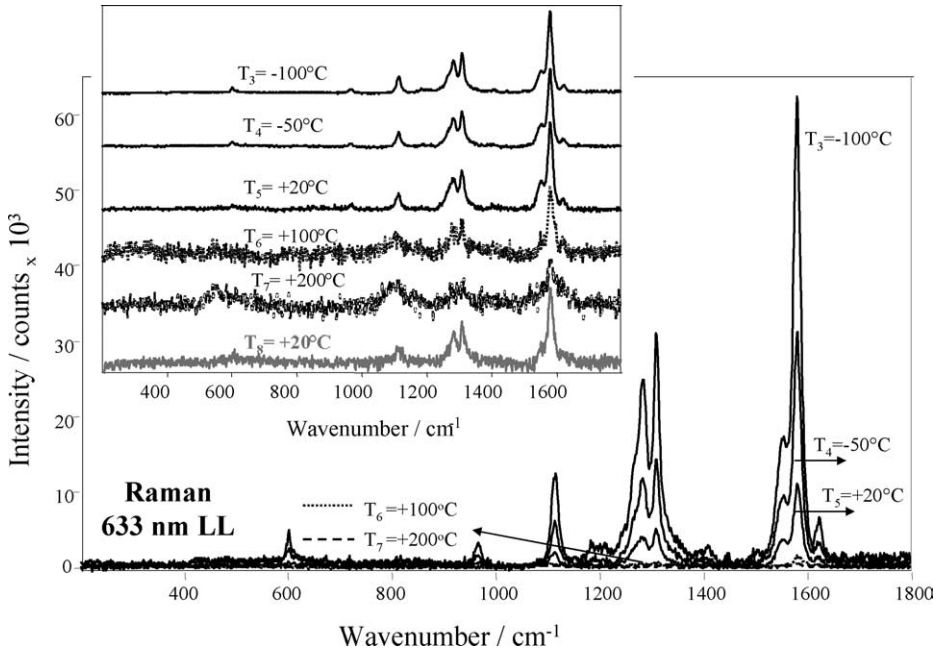

Fig. 8. Raman spectra obtained with the 633 nm laser line for the 25-layer LB film submitted to the same temperature program commented in Fig. 7 (the spectra for $T_1 = +20$ °C and $T_2 = -50$ °C are not presented since they are very similar to T_5 and T_4, respectively). The inset blows up the spectra from T_3 to T_8.

were performed on an interdigitated chromium–gold array. The conductivity increases from 0.2 nS m^{-1} under dark to 0.4 nS m^{-1} under an illumination of 152 mW cm^{-2}, as shown in Fig. 10(a) for an 81-layer LB film. These numbers indicate poor photoconduction due to the insulating characteristics of OC_1OC_{18}-PPV. This conductivity in the dark, for instance, is typical of undoped semiconductors [25], being ca. two orders of magnitude lower than for LB films of OC_1OC_6-PPV (a very similar PPV derivative but with a shorter side chain). The lower conductivity is probably associated with a different molecular arrangement of the polymer in the LB film (packing and anisotropy), in addition to the chain length. Rakhamanova and Conwell [26] showed that ordered regions should have smaller spacing and correspondingly larger polarization energy, leading to lower site energy. Also, more ordered regions generally have longer conjugation lengths. One should therefore expect that the LB films of OC_1OC_{18}-PPV, which are isotropic in relation to the LB films of OC_1OC_6-PPV [13,14], as observed experimentally. The current vs. voltage curve for a 51-layer LB film of OC_1OC_{18}-PPV is shown in Fig. 10(b), which is a typical behaviour for PLED devices. The threshold voltage is ca. 18 V and V_{onset} is ca. 23 V and, at which one can see with naked eyes a red light emitted from the device (results not shown). The absence of order in these films—as commented upon above—leads to a worsening in device performance. Indeed, V_{onset} is about three times higher than for OC_1OC_6-PPV PLEDs with the same structure [15]. A comparison between the two polymer derivatives points unequivocally to the importance of molecular ordering in the LB films for efficient PLEDs to be fabricated. In Scheme 1 are depicted possible structural arrangements for the LB films, the anisotropic OC_1OC_6-PPV and the isotropic OC_1OC_{18}-PPV, which are consistent with the experimental data reported in this paper and in ref. [13].

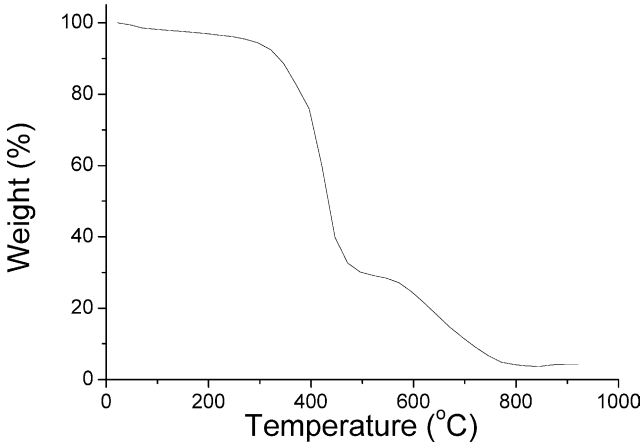

Fig. 9. Thermogravimetric curve for OC_1OC_{18}-PPV.

4. Conclusions

Stable Langmuir monolayers of OC_1OC_{18}-PPV were formed at the air/water interface, and Langmuir-Blodgett (LB) films were fabricated on solid substrates. With the long alkyl chain the monolayers were stable and amenable to transfer, but the resulting LB films displayed no spatial anisotropy. The random distribution of molecular units was confirmed by the results of several techniques, including UV–vis absorption spectroscopy, fluorescence

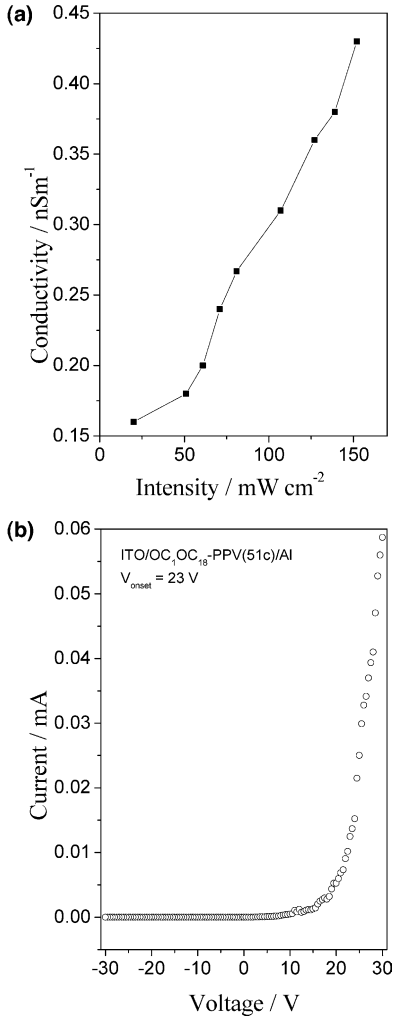

Fig. 10. Conductivity vs. intensity under different illumination conditions for an 81-layer LB film of OC_1OC_{18}-PPV (a); and current vs. voltage for a 51-layer LB film of OC_1OC_{18}-PPV (b).

spectroscopy, FTIR and Raman scattering. Thermal stability studies indicate that the LB films can withstand temperatures in the range between −100 and +100 °C. The lack of organization of the polymer molecules result in a photoconductivity efficiency considerably lower than for LB films of another PPV derivative with a shorter-chain OC_1OC_6-PPV. As a consequence, PLEDs fabricated with OC_1OC_{18}-PPV exhibited lower performance, in terms of operating voltage, than their counterparts made with OC_1OC_6-PPV. In future work, PPV derivatives with alkyl chains of intermediate length will be studied to obtain a complete picture of the effects from the lateral chain length on the anisotropy and photoconductivity of the LB films.

Acknowledgements

The authors are grateful to FAPESP, CNPq and IMMP/MCT (Brazil) and NSERC (Canada).

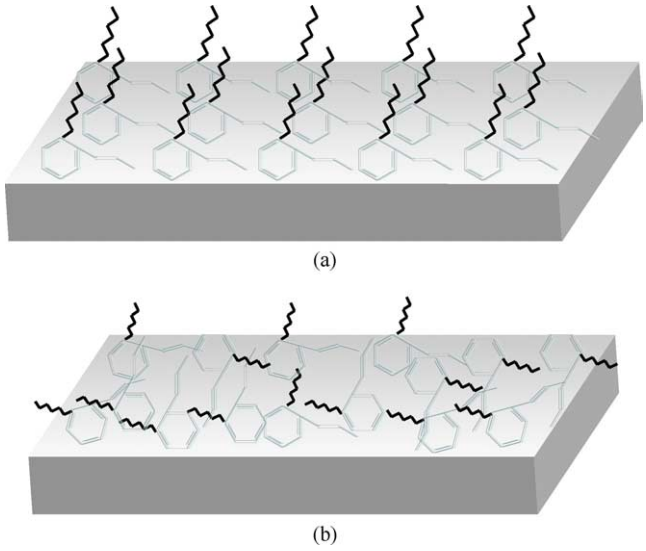

Scheme 1. Schematic diagram for the structural arrangement for (a) anisotropic LB film (OC_1OC_6-PPV) and (b) isotropic LB film (OC_1OC_{18}-PPV).

References

[1] Burroughes JH, Bradley DDC, Brown AR, Marks RN, Mackay K, Friend RH, et al. Nature 1990;39:539–41.
[2] Greenham NC, Moratti SC, Bradley DDC, Friend RH, Holmes AB. Nature 1993;365:628–30.
[3] Marconi FM, Bianchi RF, Faria RM, Balogh DT. Mol Cryst Liq Cryst 2002;374:475–80.
[4] Ferreira M, Zucolotto V, Ferreira M, Oliveira Jr ON, Wohnrath K. In: Nalwa HS, editor. Encyclopedia of nanoscience and nanotechnology, vol. 4. Los Angeles, CA: American Scientific Publishers; 2003. p. 441–65.
[5] Sluch MI, Pearson C, Petty MC, Halim M, Samuel IDW. Synth Met 1998;94:285–9.
[6] Wu ZK, Wu SX, Liao JH, Fu DG, Liang YQ. Synth Met 2002;130: 35–8.
[7] Wu ZK, Wu SX, Liang Y. Langmuir 2001;17:7267–73.
[8] Jung GY, Pearson C, Horsburg LE, Samuel IDW, Monkman AP, Petty MC. J Phys D: Appl Phys 2000;33:1029–35.
[9] Jung GY, Pearson C, Kilitziraki M, Horsburgh LE, Monkman AP, Samuel IDW, et al. J Mater Chem 2000;10:163–7.
[10] Kalinowski J. J Phys D: Appl Phys 1999;32:R179–R250.
[11] McBranch D, Campbell IH, Smith DL. Appl Phys Lett 1995;66: 1175–7.
[12] Marletta A, Gonçalves D, Oliveira Jr. ON, Faria RM, Guimarães FEG. Macromolecules 2000;33:5886–90.
[13] Ferreira M, Constantino CJL, Olivati CA, Vega ML, Balogh DT, Aroca RF, et al. Langmuir 2003;19:8835–42.
[14] Olivati CA, Ferreira M, Cazati T, Balogh DT, Guimarães FEG, Oliveira Jr. ON, et al. Chem Phys Lett 2003;381:404–9.
[15] Olivati CA, Ferreira M, Carvalho AJF, Balogh DT, Oliveira Jr ON, Seggern HV, et al. Chem Phys Lett 2005;408:31–6.
[16] Petty MC. Langmuir-Blodgett films—an introduction. Cambridge: Cambridge University Press; 1996.
[17] Olivati CA, Bianchi RF, Marconi FM, Balogh DT, Faria RM. Mol Cryst Liq Cryst 2002;374:451–6.
[18] Marletta A, Piovesan E, Dantas NO, de Souza NC, Olivati CA, Balogh DT, et al. J Appl Phys 2003;94:5592–8.
[19] Rikukawa M, Rubner MF. Langmuir 1994;10:519–24.
[20] Weitz DA, Garoff S, Nitzan A. J Chem Phys 1983;78:5324–38.

[21] Antunes PA, Constantino CJL, Aroca RF. Langmuir 2001;17: 2958–64 [and refs therein].
[22] Sakamoto A, Furukawa Y, Tasumi M. J Phys Chem 1992;96:1490–4.
[23] Antunes PA, Constantino CJL, Duff J, Aroca R. Appl Spectrosc 2001; 55:1341–6 [and refs therein].
[24] Tzung-Fang Guo, Yang Y. Appl Phys Lett 2002;80:148–50.
[25] Friend RH. Physics and chemistry of electrons and ions in condensed matter. Dordrecht, Netherlands: D. Reidel Publishing Company; 1984 p. 625–51.
[26] Rakhmanova SV, Conwell EM. Synth Met 2001;(111):389–91.